Atomic Spectroscopy

July/August 2002   Volume 23, No. 4

In This Issue:

**Issues also
available
electronically.**

(see inside front cover)

PerkinElmer™
instruments.

Determination of Chlorine, Fluorine, Bromine, and Iodine in Coals with ICP-MS and I.C.

*M. Bettinelli, S. Spezia, C. Minoia, and A. Ronchi
Laboratory of Environmental Hygiene and Industrial Toxicology
Salvatore Maugeri Foundation, via Alzaia 29, Pavia, Italy

INTRODUCTION

In order to generate electricity, fuels are combusted at high temperatures in utility boilers. This process releases many organic and inorganic pollutants into the atmosphere, both in gaseous and solid form (absorbed on suspended particulate).

Limiting pollutant emissions into the environment is therefore one of the main goals for the management, as well as a precise requirement, of national acts. The emission of halogens is regulated by the Italian legislation according to the DM 1277/90 n. 51 "Linee guida per le emissioni inquinanti…" which fixes (in the case of power plants) 100 mg/Nm^3 (cubic meters calculated under normal conditions of 0°C and 1013 mbar) as the limit value for Cl, and 5 mg/Nm^3 for F and Br (expressed as hydrofluoric and hydrobromic acid, respectively). No limit for iodine emissions has been established.

The emission of halogens from coal combustion depends on a number of factors:

1. The initial halogen content in coal and the chemical form in which they are present.

2. The combustion conditions (temperature and length of time in the boiler).

3. The use of various pollution control technologies.

During coal combustion in thermal power plants, chlorine, fluorine, bromine, and iodine are mainly volatilized during the combustion process (85–90%) and

*Corresponding author.
e-mail: igamb@fsm.it
Tel: +39 0382 592327
Fax: +39 0382 592072

ABSTRACT

The combustion process releases many organic and inorganic pollutants into the atmosphere, both in gaseous and solid form. During coal combustion in thermal power plants without pollution control equipment, chlorine, fluorine, bromine, and iodine present in coals are mainly volatilized as gaseous compounds. It has been estimated (1) that 94% of the chlorine in coal is volatilized, generally being emitted as gaseous HCl. Emission values of 99% for chlorine, 90% for fluorine, 60% for bromine, and 90% for iodine have been given for pulverized coal combustion based on actual measurements at the 600 Mwe power station in Netherlands (2).

Limiting pollutant emissions is a precise requirement of the Italian legislation that fixes (in the case of power plants) 100 mg/Nm^3 as the limit value for chlorine, and 5 mg/Nm^3 for fluorine and bromine (expressed as hydrofluoric and hydrobromic acid, respectively). No limit for iodine emissions has been established.

From this point of view and in order to maintain control of emissions from combustion plants, it is important to monitor the concentration of halogens in fuels. Unfortunately, in literature there are very few data published with regard to the amount of halogens in fossil fuels, which emphasizes the analytical difficulties with regard to the determination of these analytes.

In the present paper, a pyrohydrolysis of the sample at 1100°C, followed by the absorption of volatilized compounds in Na$_2$CO$_3$/NaHCO$_3$ solution and the final instrumental analysis of Cl, Br, and F with ion chromatography (IC) and Br and I with inductively coupled plasma mass spectrometry (ICP-MS) has been adopted.

The accuracy of the method, evaluated by analyzing some certified reference materials, was better than 95% for all analytes and the detection limits adequate to the analytical requirements (0.1 mg/kg for Br and I, 1 mg/kg for F, and 10 mg/kg for Cl).

remain in the fumes downstream of the ash abatement equipment (electrostatic precipitators) as gaseous compounds, particularly as acids.

Experimental studies on a "pulverized dry-bottom" boiler, equipped with high-efficiency electro-filters and stoked with bituminous coal, showed a distribution ratio higher than 90–95% in the vapor phase for chlorine and bromine, 80–85% in the case of fluorine, and 75–80% for iodine (3).

If no desulphurization plant is present, the majority of halogens introduced with the fuels are emitted at the stack and the concentration in the flue gases is strictly related to the initial concentration of these elements in fuels.

In the case of plants equipped with wet gas desulphurization systems (wet FGD), the gas scavenging in the pre-scrubber can lead to a significant reduction of chlorine, bromine, and iodine concentration in the gaseous phase (more than 90%), while the removal ratio of fluorine seems to be less efficient (rate of 50%).

From this point of view, and in order to maintain control of combustion plant emissions, it is important to monitor the concentration of halogens in fuels.

In the literature there are very few data published with regard to the amount of halogens in fossil fuels or in environmental matrices, emphasizing the analytical difficulties in the determination of these analytes.

The conversion of Cl, F, Br, and I compounds for analysis in coal in a convenient form is widely considered a crucial analytical step.

Based on work in the past, a method for fluorine analysis (ASTM D 3761-84) was published by ASTM. It consists of sample combustion in a calorimetric bomb, absorption of the produced gases by means of a NaOH solution, and final fluoride analysis with ISE (4).

The US Geological Survey (5) uses a method based on sample incineration at 525°C and melting of the ashes with MgO and $MgNO_3$. ISO has recently reported a method for total fluorine determination by means of ISE or IC after pyrohydrolysis of the sample in an oven (6).

There is only one official method that was published by ASTM (ASTM D 4208-88) for chlorine determination in fossil fuels. It is based on bomb combustion and ISE analysis, while there are none published for other halogens.

Very few studies have been reported with regard to fuel halogen analysis, and the majority of these use combustion in a calorimetric bomb for the sample preparation steps (7,8), alkaline fusion with several melting agents (NaOH, NaOH / MgO, NaOH / $MgO+MgNO_3$, Na_2CO_3, etc.) (9), furnace induction heating (10), pyrohydrolysis (11–13), all of them followed by ISE or IC analysis.

Some papers moreover report analyses with specific techniques such as PIGE (14), NAA (15), and ICP-MS (16,17).

Based on these considerations, the importance of developing a method for the accurate determination of halogens in coals is evident. In the present paper, a pyrohydrolysis of the sample at 1100°C, followed by the absorption of volatilized compounds in Na_2CO_3/$NaHCO_3$ solution and the instrumental analysis of Cl, Br, F with ion chromatography (IC) and Br and I with inductively coupled plasma

mass spectrometry (ICP-MS) has been adopted.

The accuracy of the method was evaluated analyzing the following certified reference materials: NIST 1632b Trace Elements in Coal; NIST 1633a Trace Elements in Coal Fly Ash; BRC 60 Chlorine and Fluorine in coal; MURST-ISS-A1 Antarctic Marine Sediment CRM for Trace Elements; and NIST 1573a Tomato Leaves. The good recovery obtained for all the CRMs analyzed confirmed the applicability of this procedure, even to the characterization of environmental matrices (sediments and biological materials) not reported in this paper.

EXPERIMENTAL

Instrumentation

ELAN® 5000 ICP-MS (PerkinElmer Sciex Instruments, Concord, Ontario, Canada), equipped with two mass-flow controllers, Ryton® spray chamber, GemTip™ cross-flow nebulizer, and a PerkinElmer AS-90 autosampler (PerkinElmer, Shelton, CT USA).

Dionex DX-100 ion chromatograph (Dionex Corporation, Sunnyvale, CA, USA), equipped with an AS-9HC analytical column (high capacity alkyl/alkanol quaternary ammonium), guard column AG-9HC, DXP-Dionex analytical pump, and ASRS-Ultra autoregenerant conductivity suppressor.

GAAM Combustor 02 combustion furnace (GAAM mbH, Bad Durrenberg, Germany).

Reagents and Standard Solutions

Nitric acid (65% m/v) was Suprapur® reagent (E. Merck, Darmstadt, Germany).

Multielemental standard solutions were prepared from 1000 mg/L single-element reference standards (Merck) by dilution in water.

High-purity water produced by passing distilled water through a deionizing system (Milli-Q™, Millipore, Bedford, MA, USA).

Sodium carbonate (Na_2CO_3) of analytical reagent grade (Carlo Erba).

Sodium bicarbonate ($NaHCO_3$) of analytical reagent grade (Carlo Erba).

Certified Reference Materials

The following certified reference materials were analyzed:

NIST 1632b Trace Elements in Coal

NIST 1633a Trace Elements in Coal Fly Ash

BCR 460 Chlorine and Fluorine in Coal

MURST-ISS-A1 Antarctic Marine Sediment CRM for Trace Elements

NIST 1573a Tomato Leaves

Sample Preparation

A sample of 0.5 g, previously dried for one hour in an oven at 60°C, was introduced into a quartz combustion tube of the GAAM tubular oven and heated at about 1000°C.

The GAAM combustor allows full control of the heating process by on-line monitoring of the combustion rate and the automatic variation of the introduction speed of the sample.

During the heating process, a humidified gas (first step with argon, second step with oxygen) was blown into the tube in order to promote pyrohydrolysis of the sample.

The combustion products were collected in two quartz impingers filled with 20 mL of an alkaline absorption solution (Na_2CO_3 1.8 mM / $NaHCO_3$ 1.7 mM), then diluted with water to a final volume of 50 mL, and analyzed by IC (F, Cl, and Br) or ICP-MS (Br and I).

The instrumental parameters are listed in Tables I-III.

RESULTS AND DISCUSSION

F and Cl Determination

The results for the CRM previously cited and reported in Table IV were in good agreement with the certified or indicative values (recoveries between 93–101%) with the exception of fluorine in NIST 1633a (reported value 94 ± 20 µg/g, found value 75 ± 2 µg/g). Our result was, in any case, very similar to that reported by Rice (10) on the same material (73 ± 2 µg/g), thus confirming as "suspected" the value reported by NIST.

The long-term precision was evaluated by analyzing the same certified reference materials on 15 different days (over the course of a year) and drawing the respective control charts, as shown for chlorine in Figure 1.

The long-term precision for samples containing about 50 mg/kg of Cl and F was in the order of 19–20%, while for higher concentrations (225 mg/kg F and 1083 mg/kg Cl), a precision of 5% was found.

Br and I Determination

Since the majority of reference materials have no certified values, only indicative values, the accuracy for Br and I was confirmed by evaluating the recovery in coal samples spiked with known concentrations of halogens (see Table V). Four concentration levels were tested (10, 100, 500, and 1000 mg/kg) and the recoveries were in the range 99.7 – 106.6 % for bromine and 89.5 – 101.6 % for iodine.

Moreover, a comparison between the results obtained in the analysis of coal samples by ICP-MS, ion chromatography (I.C.), and neutron activation analysis (NAA) was performed. The results

TABLE I
ICP-MS Instrumental Parameters

Parameters	
RF Power	1150 W
Ar Plasma Flow	15.0 L/min
Ar Nebulizer Flow	0.90 L/min
Ar Auxiliary Flow	1.0 L/min
Sample Flow	1 mL/min
Nebulizer	Cross-flow
Reading	Peak hopping
Resolution	Normal
Dwell time	150 ms
Sweeps / Replicates	5
Number of Replicates	5
Calibration Curve	Linear through zero
Calibration Points	3 (10 – 50 – 100 µg/L)
Isotopes	79Br, 81Br, 127I

TABLE II
I.C. Instrumental Parameters

Column	AS9-HC
Pre-column	AG9-HC
Eluent	Na_2CO_3 9.0 mM
Eluent Flow	1.0 mL/min
Injection Loop	75 µL
Suppressor	ASRS-ULTRA
Calibration Curve	Quadratic
Calibration Points	7 – with the following ranges:
	F 0.25 – 5 mg/L
	Cl 0.25 – 10 mg/L
	Br 0.50 – 20 mg/L
Retention Times	F 4.08 min
	Cl 6.92 min
	Br 11.12 min
Data Processing	Peak Area

TABLE III
GAAM Oven Instrumental Parameters

Oven Temperature	1080°C	
Step 1	Time	180 s
	Ar Flow	35 L/h
	Oxygen Flow	40 L/h
Cooling Time	60 s	
Step 2	Time	300 s
	Oxygen Flow	90 L/h
Absorption Solution	Na_2CO_3 1.8 mM - $NaHCO_3$ 1.7 mM	

TABLE IV
Comparison Between Chlorine and Fluorine Concentrations (µg/g)
Certified and Measured After Pyrohydrolysis of Sample and Analysis With Ion Chromatography

CRM	Chlorine (µg/g)		Fluorine (µg/g)	
	Certified Value	Found Value	Certified Value	Found Value
NIST 1632b	1260	1192 ± 9	50 ± 6	45.7 ± 3.3
BCR 460	59 ± 8	57 ± 8	225 ± 6	232 ± 9
NIST 1633a	< 69	38 ±3	94 ± 20[a]	75 ± 2
MURST-ISS-A1	7385 – 7800	6825 ± 70	-	125 ± 3
NIST 1573	1.07 ± 0.03 (%)	1.03 ± 0.04 (%)	5.5 ± 0.4	5.2 ± 0.2

[a] Value reported from Rice (12) 73 ± 2 µg/g.

TABLE V
Comparison Between Bromine and Iodine Concentrations (µg/g) Certified and Measured
After Pyrohydrolysis of Sample and Analysis With Ion Chromatography

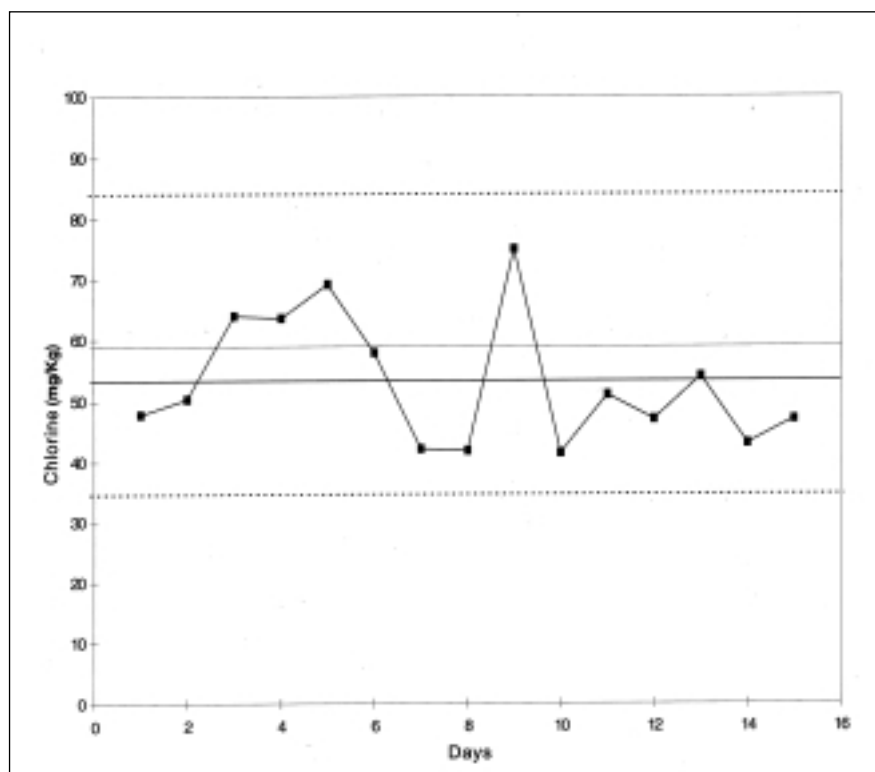| CRM	Bromine (µg/g)		Iodine (µg/g)	
	Certified Value	Found Value	Certified Value	Found Value
NIST 1632b	17	15.2 ± 1.0	--	1.80 ± 0.05
NIST 1633a	2.3	2.1 ± 0.3	< 4.5	1.5 ± 0.8
MURST-ISS-A1	34.9 – 50.5	38.2 ± 0.2	34.6 – 42.3	36.0 ± 0.3
NIST 1573	21 ± 2	23 ± 2	0.323 ± 0.058	0.42 ± 0.07

Fig. 1. Control chart for chlorine determination in BCR 460 certified reference material (certified value 59 ± 8 mg/kg; found value 57 ± 8 mg/kg; mean and standard deviation were obtained on 15 different working days).

reported in Figures 2 and 3 show good agreement between the techniques considered. (The correlation curves in the case of 51 bromine analyses done by IC and ICP-MS gave a value of $R^2 = 0.9661$ with intercept a= 1.2151 and slope b= 0.9689; while for 34 iodine analyses performed by ICP-MS and NAA, the same statistical parameters were: $R^2 = 0.9902$, a= 0.4956, b= 0.9007 and 0.9902).

Method detection limits (MDLs), calculated as three times the standard deviation of 10 repeated analyses of a blank treated as the samples, were 0.1 mg/kg for Br and I, 1 mg/kg for F, and 10 mg/kg for Cl. These MDLs appear adequate for the determination of these elements in many matrices of environmental interest.

The procedure described in this paper was adopted to monitor, on a routine basis, the halogen content in a series of coals imported to Italy from different countries.

The results reported in Tables VI-IX and the knowledge of the emission factors reported in the literature for power plants,
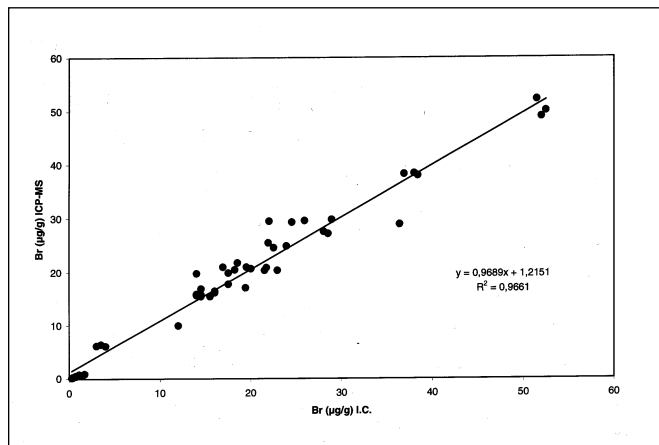
Fig. 2. Bromine - Comparison between I.C. and ICP-MS results after hydropyrolytic treatment of coal samples (n= 51; a = 1.2151 ; b = 0.9689; R^2 = 0.9661).

Fig. 3. Iodine - Comparison between ICP-MS (after hydropyrolytic treatment of coal samples) and NAA results (n = 34; a = 0.4956; b = 0.9007; R^2 = 0.9902).

equipped with different post-combustion pollution control equipment, can be utilized to predict the halogen emissions and thus also establish the major sources of these compounds in the atmosphere.

CONCLUSION

The accurate analysis of halogens in coals and environmental matrices is a difficult task as evidenced by the relative lack of data reported in the literature.

In this paper, a method has been described for the determination of Cl, F, Br, and I in coals, sediment, and botanic materials.

The method was validated by analyzing certified reference materials, evaluating the recoveries of the analytes in spiked real samples, and comparing the results with independent techniques such as NAA.

The method detection limits (0.1 mg/kg for Br and I, 1 mg/kg for F, and 10 mg/kg for Cl) were adequate for the determination of these elements in many matrices of environmental interest.

The procedure described in this paper was adopted to analyze more than 200 coals of different origin and a database of halogen concentrations is now available.

TABLE VI
Fluorine Content of Various Coals Imported to Italy

Place of Origin	Sample No.	Mean (mg/kg)	Standard Deviation (mg/kg)	Median (mg/kg)	Range (mg/kg)
COLUMBIA	15	37	8	36	34–46
POLAND	15	91	17	83	61–107
USSR	8	122	10	119	115–139
SOUTH AFRICA	22	241	57	232	175–380
USA	52	63	30	55	36–241
VENEZUELA	8	29	3	27	26–34
TOTAL	120	111	86	66	26–380

TABLE VII
Chlorine Content of Various Coals Imported to Italy

Place of Origin	Sample No.	Mean (mg/kg)	Standard Deviation (mg/kg)	Median (mg/kg)	Range (mg/kg)
CHINA	15	430	7	434	413–456
COLUMBIA	15	255	209	149	70–579
POLAND	15	1089	167	1057	851–1343
USSR	8	70	35	73	29–99
SOUTH AFRICA	23	66	13	61	37–86
USA	113	1347	548	1228	96–2692
VENEZUELA	8	231	116	292	83–295
TOTAL	196	1035	676	1069	29–2692

TABLE VIII
Bromine Content of Various Coals Imported to Italy

Place of Origin	Sample No.	Mean (mg/kg)	Standard Deviation (mg/kg)	Median (mg/kg)	Range (mg/kg)
CHINA	15	4.4	2.1	4.7	2.45–7.21
COLUMBIA	15	2.5	0.7	2.2	1.64–3.92
POLAND	4	11.5	0.7	12.1	10.9–13.3
SOUTH AFRICA	39	1.3	1.0	1.1	0.38–5.8
USA	76	19.9	7.0	17.4	5.1–43.2
VENEZUELA	10	1.8	0.6	1.7	1.65–3.11
TOTAL	159	11.6	9.9	11.5	0.37–42.5

TABLE IX
Iodine Content of Various Coals Imported to Italy

Place of Origin	Sample No.	Mean (mg/kg)	Standard Deviation (mg/kg)	Median (mg/kg)	Range (mg/kg)
CHINA	15	2.9	2.9	2.9	0.78–5.3
COLUMBIA	15	1.1	0.4	0.8	0.85–1.63
POLAND	4	4.1	2.9	2.5	2.3–7.7
SOUTH AFRICA	28	1.2	0.8	1.1	0.15–2.76
USA	86	3.1	1.7	2.6	0.38–12.8
VENEZUELA	10	1.8	0.8	1.5	0.9–3.8
TOTAL	158	2.8	1.7	2.4	0.15–12.8

REFERENCES

1. T.L. Japalucci, R.J. Demski, and D. Bienstock, Chlorine in coal combustion, US Bureau of Mines, Report of Investigations, USBMRI7260, Pittsburg, PA, USA (1969).

2. R. Meij, Personal Communication, Arnhen, The Netherland, KEMA (March 1991).

3. R. Meij, Tracking trace elements at a coal-fired power plant equipped with a wet flue-gas desulphurization facility, KEMA Scientific and Technical Reports, Special Issue, 7, 267 (1989).

4. ASTM D 3671-84, Test method for total fluorine in coal by oxygen bomb combustion / ion selective electrode method, 1989 Annual Book of ASTM Standard, Volume 05.05 Gaseous Fuels, Coals and Coke.

5. D.W. Golightly and F.O. Simon, US Geological Survey Bulletin 1823, 72 (1989).

6. ISO / DIS 11724 , Solid mineral fuels – Determination of total fluorine (1996).

7. R.A. Nadkarni, Am. Lab. 13, 22 (1981).

8. R.A. Nadkarni and D.M. Pond, Anal. Chim. Acta 146, 261 (1983).

9. P. Schramel and S. Hasse, Mikrochim. Acta 116, 205 (1994).

10. T. Shinonaga, M. Edibhara, H. Nakahara, K. Tomura, and K.G. Heumann, Chemical Geol. 115, 213 (1994).

11. M. Bettinelli, Analyst 108, 404 (1983).

12. T.D. Rice, Talanta 35, 173 (1988).

13. M. Langenauer, U. Krahenbuhl, and A.Wyttenbach, Anal. Chim. Acta 274, 253 (1993).

14. V.B. Conrad and W.B. Brownlee, Anal. Chem. 60, 365 (1988).

15. I. Roelandts, G. Robaye, J.M. Delbrouck-Harabu, and G.Weber, Talanta 43, 439 (1996).

16. Y. Muramatsu and S. Yoshida, J. Radioanal. Nucl. Chem. 197, 149 (1987).

17. K.G. Heumann and H. Seewald, Fresenius' Z. Anal. Chem. 329, 485 (1987).

18. B. Schnetger and Y. Muramatsu, Analyst 121, 1627 (1996).

Marine Sediment Analysis Using Inductively Coupled Plasma Optical Emission Spectrometry

*Dirce Pozebon and Patrícia Martins**
Instituto de Química, Universidade Federal do Rio Grande do Sul
Av. Bento Gonçalves, 9.500 - 91.501-970, Porto Alegre, RS, Brazil

INTRODUCTION

For geological and environmental studies, it is important to know the composition and contamination of marine sediments. Due to the complexity of the sample matrix, several methods of sample decomposition have been studied and proposed. In some cases, incomplete sample decomposition may occur, lowering precision, accuracy, and analytical results (1–3).

Methods using acid decomposition and heating in open flasks (4), polytetrafluorethylene (3,5) (PTFE) closed vessels under pressure (pumps), and microwave oven (2,6) have largely been employed. For trace element determination, sample decomposition in closed vessels is recommended in order to avoid analyte losses and contamination. In these methods, used for marine sediment decomposition, problems such as analyte volatilization, precipitation, and incomplete sample solubilization may occur (1). When acid digestion is used, solubilization efficiency depends on the sediment sample characteristics, acid type, acid mixture, and temperature (1,7). The extraction of some elements such as Fe, Cr, Ti, Mg, and Al from sediments is sometimes difficult as they are present as oxides, phosphates, and silicates which are refractory species (2,3). Due to this fact, alkaline fusion may be necessary for complete sample solubilization in order to obtain accurate results.

_____
Corresponding author.
e-mail: dircepoz@iq.ufrgs.br
Fax: +55-51- 33167304

ABSTRACT

A method is described for the ICP-OES determination of Al, As, Cd, Co, Cr, Cu, Ba, Fe, Mn, Ni, Pb, V, and Zn in marine sediments. An ICP-OES instrument equipped with a dual-view plasma torch was used. This technology allows the determination of trace elements in the axial view mode along with major components in the radial view. The radial and axial views and the sample preparation procedure as acid digestion and alkaline fusion were investigated in order to obtain accurate results for all analytes. External calibration was used to determine the analytes in sample acid digestion or in alkaline fusion sample solution. For Cd determinations, matrix matching with As and V was used. More precise and accurate results for Ba and Al were found when the sediment was fused instead of acid-digested. Sample solutions containing a high content of acids (HCl, HF, and HNO_3) and dissolved solids (provided by alkaline fusion) could be analyzed. However, some analytes could only be correctly determined using the radial view mode. Parameters like LOD (limits of detection) and % RSD (relative standard deviation) are presented. The method was applied to the analysis of real marine sediment samples.

Several spectroscopic techniques have been used for the determination of trace and major elements in marine sediments. Among the most used spectroscopic techniques are inductively coupled plasma mass spectrometry (ICP-MS) (8,9), inductively coupled plasma optical emission spectrometry (ICP-OES) (9,10), flame atomic absorption spectrometry (FAAS) (11), graphite furnace atomic absorption spectrometry (GFAAS) (12,13), and X-ray fluorescence (XRF) (14). ICP-MS and GFAAS have been the most selected techniques for trace element determination in environmental samples. ICP-MS, due to its multielement detection feature, low spectral interferences for a great number of elements, large dynamic calibration range, and high sensitivity, is the preferred technique. The use of ICP-OES for trace element determination is also reported (9,10). With the more recent ICP-OES instruments using charge coupled device detectors (CCD) with automatic dual view, it is possible to obtain low limits of detection (LOD). The quantum efficiency achieved with CCD is higher than it is for the photomultipliers (PMT), thus improving sensitivity. When using axial view, the sensitivity may also be improved but matrix effects are more pronounced in comparison to radial view. However, as reported (15–17) this matrix effect may be minimized by using robust plasma conditions such as high power and low nebulizer gas flow rates. Besides, in comparison to ICP-MS, ICP-OES is less prone to matrix interferences. Therefore, it is possible to introduce relatively concentrated acid mixtures into the plasma (7) as well as solutions

containing high amounts of dissolved solids since a feasible system for sample introduction is also available.

The main purpose of this work was to develop a method for As, Co, Cr, Cu, Ni, Pb, V, Al, Fe, Cd, Zn, Mn, and Ba determination in marine sediments by ICP-OES. Various sample decomposition methods were investigated as well as instrumental parameters.

EXPERIMENTAL

Intrumentation

All determinations were performed using the scanning Optima™ 2000 DV ICP-OES (PerkinElmer, Shelton, CT, USA) equipped with a three-channel peristaltic pump. The parameters used are listed in Tables I and II. These parameters were optimized or used as recommended by the instrument manufacturer.

Reagents and Standard Solutions

All reagents used were of analytical grade. The acids used were 65% (v/v) HNO_3, 37% (v/v) HCl, 40% (v/v) HF, and 30% (v/v) H_2O_2 (Merck, Darmstadt, Germany). HNO_3 and HCl, doubly distilled in sub-boiling quartz steam (Hans Kürner, Rosenheim, Germany), were used for sample decomposition and calibration solutions. Milli-Q™ (Bedford, MA, USA) water (resistivity of 18.2 $M\Omega$.cm) was used for all solutions and for sample preparation. This water was also used to rinse the vessels used to store the solutions for samples. Calibration solutions were prepared by dilution of a multielement 1000 mg L^{-1} (ICP - IV from Merck) stock solution or from 1000 mg L^{-1} single-element stock solutions (Titrisol®, Merck) mixed with 5% (v/v) HNO_3 solution. For alkaline sediment fusion, $Na_2B_4O_7 \cdot 7H_2O$ (Merck) was used.

TABLE I
Instrumental Operating Conditions

Plasma power	1300–1500 W	Resolution	High
Plasma gas flow	15 L min^{-1}	Spectral profiling	No
Auxiliary gas flow	0.2 L min^{-1}	Integration time	auto, min. 1 sec, max. 5 sec
Nebulizer gas flow*	0.6 L min^{-1} and 0.7 L min^{-1}	Read delay	10 sec
Nitrogen purge	normal	Sample flow	2.5 mL/min
Height of observation	15–16 mm	Sample flush	10 sec
Nebulizer	GemCone™	Injector	Alumina (aluminum oxide) 2 mm
Nebulizer chamber	Scott (Ryton®)	Replicates	2
Processing mode	Area (7 points per peak)	Background correction	Two points

*For Ba and Cd determinations, a flow rate of 0.80 L min^{-1} was used; 0.6 L min^{-1} using axial view and 0.7 L min^{-1} using radial view.

TABLE II
Spectral Lines, Calibration Solutions Concentration, and Background Correction

Analyte	Spectral line (nm)	View	Range of concentrations* (μg L^{-1})	Background correction BCG1	BCG2
As(I)	188.979	Axial	20 - 100	-0.010	0.022
Co(II)	231.161	Radial	20 - 100	-0.009	0.010
Cr(II)	267.716	Radial	50 - 400	-0.019	0.026
Cu(I)	324.752	Radial	40 - 150	-0.020	0.021
Ni(II)	231.604	Axial/Radial	50 - 250	-0.013	0.016
Pb(II)	220.353	Axial/Radial	50 - 200	-0.016	0.016
V(II)	292.464	Radial	100 - 500	-0.029	0.026
Al(I)	396.153	Radial	2000 - 10000	-0.043	0.043
Fe(II)	239.562	Axial/Radial	2000 - 10000	-0.014	0.021
Cd(II)	228.802	Radial/Axial	1.0 – 8.0	-0.012	0.007
Zn(I)	213.857	Axial/Radial	50 - 150	-0.045	0.045
Mn(II)	257.610	Axial/Radial	50 - 250	-0.028	0.026
Ba(II)	455.403	Radial	100 - 500	-0.056	0.039

*Calibration Equations: linear through 0 for all elements.

All glassware and labware used to store the solutions were decontaminated with 10% (v/v) HNO_3 solution for 72 h. Agate mortars, polyethylene dishes, and nylon sieves were decontaminated by immersing them in 1% (v/v) HNO_3 for 24 h. After immersion in the acid solutions, all materials were thoroughly washed with distilled water and rinsed with Milli-Q water. The polyethylene flasks used to store the sediment samples and their solutions were previously decontaminated following this procedure: (a) mixing solution with 50% (v/v) HNO_3 solution and left standing for 1 week, (b) mixing with 3% HNO_3 (v/v) and left standing for 1 week, (c) washing with distilled water and rinsing with deionized water, and (d) drying in a Class 100 clean room at room

temperature. The Pt crucibles used for alkaline fusion were washed by immersion in 50% (v/v) HCl solution and heating at about 90ºC for 5 h.

Sample Preparation

Certified marine sediment sample PACS 2 from the National Research Council of Canada (NRCC) and real marine sediment samples from Rio de Janeiro, Brazil, were analyzed. All samples were prepared in a Class 100 clean room. The certified sample was analyzed as received, while the real samples were prepared according to the following procedure: (a) sample the sediment at a depth of about 900 m, (b) sub-sample the sediment using a decontaminated polyethylene spatula, (c) place about 200 g of the sediment in a decontaminated 250-mL polyethylene flask; (d) cap the flask and freeze the sample at about –4ºC, (e) transport the sample to the laboratory, (f) unfreeze the sample, open the flask, and let it stand in order to dry the sediment at room temperature, (g) grind the sample in an agate mortar to pass through a 2-mm nylon sieve, (f) sub-sample about 20 g of the sediment using a decontaminated polyethylene spatula and a decontaminated polyethylene dish, (g) grind the sub-sample in an agate mortar in order to pass through a 100-mm nylon sieve, and (h) store the sample in a decontaminated 30-mL capped polyethylene flask.

Three acid mixtures were investigated for the sediment sample digestions, as shown in Table III. A 0.200-g sample was placed into a PTFE pump together with an acid mixture using the same addition order as described in Table III for each mixture. Subsequently, the flask was capped and placed on a digestion block at a temperature of 160ºC for 12 h. Then, the digestion block was turned off and the solution left standing to achieve room

TABLE III
Acid Mixtures for Sample Digestion

Method	Acid Mixture
Digestion 1	Mixture 1 = 7 mL HNO_3 + 6 mL HF + 0.5 mL H_2O_2
Digestion 2	Mixture 2 = 7 mL HNO_3 + 6 mL HF + 3 mL HCl
Digestion 3	Mixture 3 = 5 mL HNO_3 + 5 mL HF + 5 mL HCl

temperature. Then, the flask was opened, the sample solution transferred to a graduated polyethylene flask, and filled to 50-mL volume. Arsenic, Cd, Pb, Cr, Ni, Cu, Cr, Zn, and V were determined directly without further sample dilution. A 20 times dilution with water was used for the Ba, Al, Fe, and Mn determinations as the concentration of these elements is relatively high in the samples. All samples as well as blanks were analyzed in triplicate.

In the alkaline fusion procedure, 0.200 g of the sample was placed in a Pt crucible followed by the addition of 1 mL HNO_3. The crucible was placed on a hot plate and heated in order to evaporate the acid. Then, 2 mL of HF was added and also evaporated. Subsequently, 2 g of $Na_2B_4O_7$ · $7H_2O$ was added and the crucible placed in a muffle. Then, the sediment sample was fused at 1000ºC for a 2-hour period. A transparent melt was produced which was removed by immersing the crucible at room temperature into 10% (v/v) HCl solution and heating to about 90ºC. Once the melt was solubilized, the crucible was taken out of the sample solution. This solution was evaporated to about 10 mL and transferred to a graduated polyethylene flask containing 1 mL HNO_3. The sample solution was diluted 20 times with water prior to introduction into the plasma.

RESULTS AND DISCUSSION

Initially, the plasma power, nebulizer gas flow rate, and observation height were optimized. The signal intensities of the elements As, Ni, Zn, Co, Pb, and Ba, present in the certified acid-digested sample, were measured and the results are shown in Figures 1 and 2. Of the elements investigated, As, Ni, Zn, Co, Pb, and Ba were selected for parameter optimization since they cover a large range of excitation and ionization energies (18). As shown in Figure 1, the best observation height and nebulizer gas flow rate with axial view was found to be 15 mm and 0.6 mL min^{-1}, respectively. These parameters were adopted for further measurements.

Because the signal intensity was higher for Ba, a 0.8 mL min^{-1} nebulizer gas flow rate was selected. It can therefore be stated that a higher aerosol introduction into the plasma is tolerated for Ba since it is one of the most easily ionizable and excited element. With regard to As, the observation height influence on its signal intensity was low and 15 mm was feasible as well as verified for the other elements.

As can be seen in Figure 1, a plasma power of 1300 W was sufficient since no significant signal increase was observed at 1500 W. However, for Cd (not shown in Figure 1) whose concentration is very low in the sample, 1500 W was adopted in order to obtain the highest signal. By comparing Figure 1 (using axial view) with Figure 2 (using radial view) it can be seen that the influences of nebulizer gas
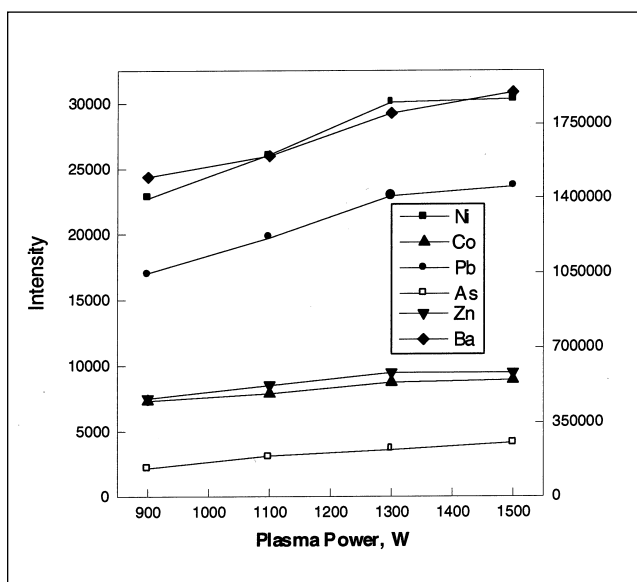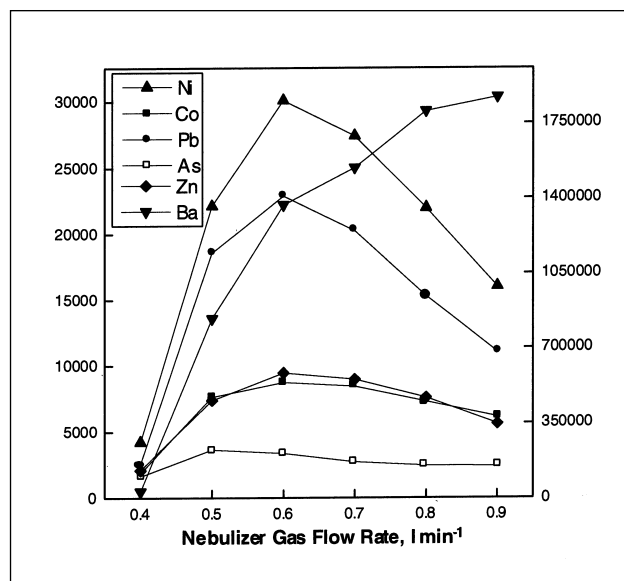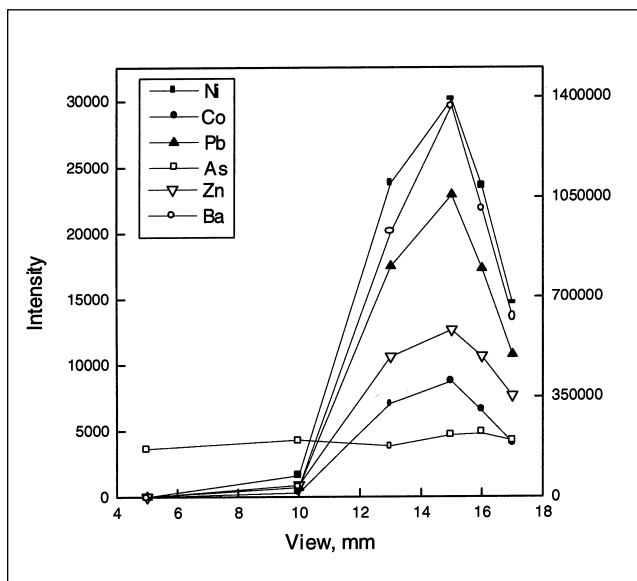
and power on the analyte signals are almost similar. In the case of the nebulizer gas, a flow rate of 0.7 mL min^{-1} was found to provide the highest signals for almost all analytes using radial view, and slightly superior signals at a flow rate of 0.6 mL min^{-1} using axial view. The Ba signal is higher at higher flow rates using both torch views. With regard to observation height, it was found that distance has little influence on the analyte signals using radial view. Based on the results obtained in Figure 2 and

the results obtained for the other analytes not presented in that figure, an observation height of 16 mm was established for use with radial view.

After optimization of the parameters as shown in Figures 1 and 2, the certified sample PACS-2 was analyzed employing the digestion methods described in Table III. Initially, the use of axial view was investigated for all analyte determinations. According to Table IV, no accurate results were obtained for almost all analytes

using digestion method 1. However, significant improvements were observed using radial view and method 1. Using digestion methods 2 or 3 and radial view, even better results were obtained for almost all analytes. It was also observed that for As, Cd, Ni, Pb, Fe, Zn, and Mn, both radial and axial view can be used. In the case of As determination, which has a low signal intensity in the analyzed sample mainly due to the element characteristics, the axial view was adopted as indicated in Table I. Table IV shows that for
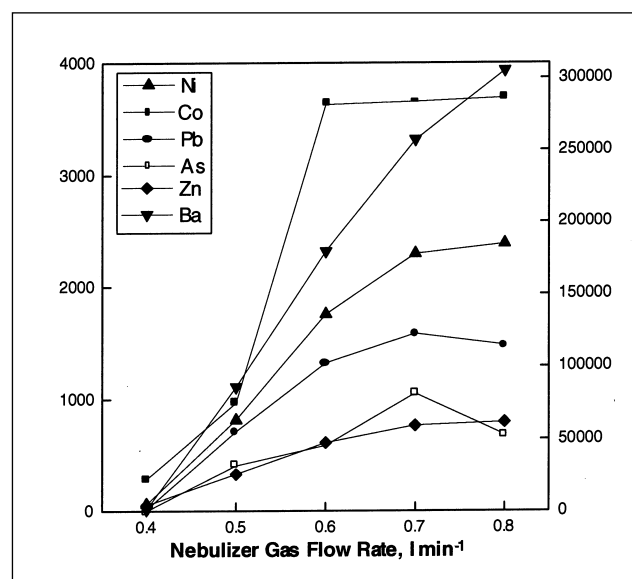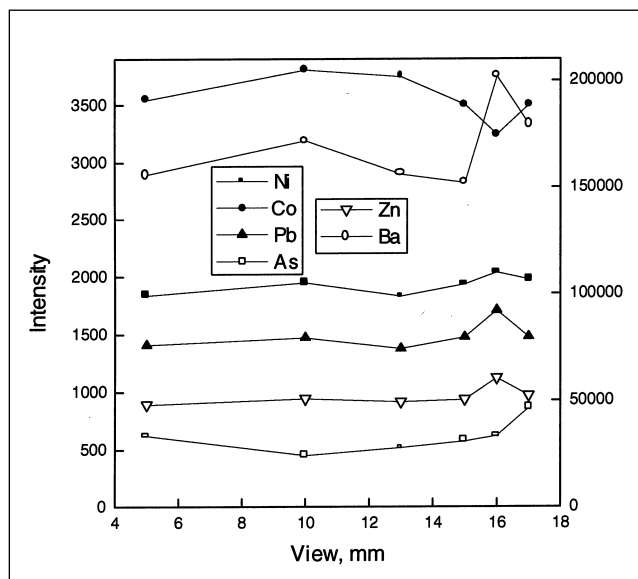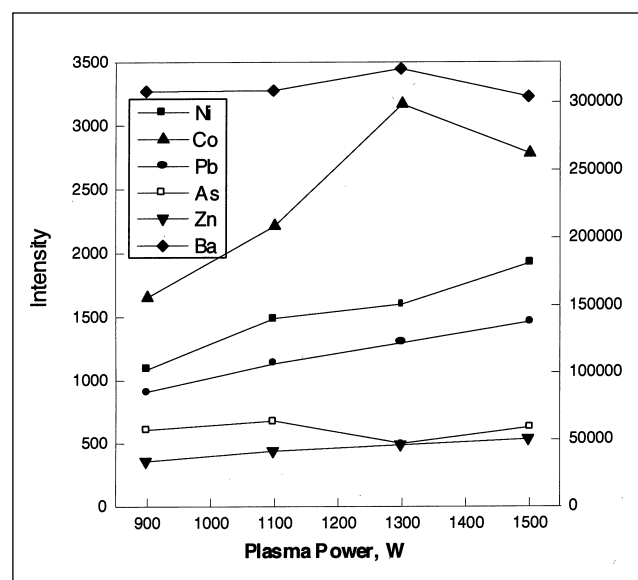
Fig. 2.
Analyte signals in marine sediment PACS -2 using radial view; the acid-digested solution sample was 5 times diluted* and 2 times diluted for other analytes. For scale adjustment, the signals of As and Co were multiplied by 2. The scale on the left is for Ni, As, Co, and Pb, whereas the scale to the right refers to Ba and Zn.

*The final sample solution (50 mL in a polyethylene volumetric flask) was diluted again prior to its introduction into the plasma (just for scale adjustment in the graphic). So, when we look at the signal intensities, we must consider that the sample was diluted (as the sample was diluted, the real signals are higher than the ones presented in Figures 1 and Figure 2).

Co the measured concentrations are always higher than the certified ones using axial view. On the other hand, the measured Co concentration is slightly lower when using radial view, but the error is low. More robust plasma conditions and other spectral lines were investigated for Co determination but it was not successful. Internal standard calibration was not investigated due to the matrix characteristics, which may contain the element used as internal standard. However, using digestion methods 2 or 3 and radial view, the error was found to be under 10% for all analytes with the exception of Al. It was observed that accurate Cd results using any sample preparation method and both observation views were only obtained using As and V matrix matching due to spectral interferences. An alternative Cd spectral line was investigated (226.502 nm) but it was also impossible to measure the analyte due to Fe spectral interferences. Consequently, the more sensitive Cd spectral line (228.802 nm) was chosen and matrix correction used.

Since no accurate results were obtained for Al and the standard deviations for Ba were high, maybe due to analyte precipitation or incomplete sample solubilization, alkaline sample fusion was investigated. As shown in Table V, better results were obtained for Al and Ba using the fusion method, which shows that the marine sediment is not always completely solubilized in relation to these two elements using acid digestion. All analytes were measured in the solution of the fused sample, but

TABLE IV

Analysis of Certified Marine Sediment Using Different Acid Digestion Mixtures (see Table III)
Results in μg g^{-1} and the spectral lines as listed in Table II were used.

Analyte	Sample Dilution	Certified	Mixture 1		Mixture 2		Mixture 3	
			Axial View	Radial View	Axial View	Radial View	Axial View	Radial View
As	none	26.2 ± 1.5	30.9 ± 8.0	23.2 ± 1.2	26.0 ± 1.7	26.0 ± 1.1	28.8 ± 1.7	27.4 ± 3.5
Co	none	11.5 ± 0.3	14.5 ± 0.7	8.17 ± 0.1	14.0 ± 0.8	9.8 ± 0.4	13.5 ± 0.3	9.6 ± 0.4
Cr	none	90.7 ± 4.6	105 ± 2.2	91.1 ± 0.9	106 ± 5.6	95.1 ±7.1	103 ± 1	101 ± 2
Cu	none	310 ± 12	391 ± 51	292 ± 1	377 ± 11	312 ± 13	340 ± 7	287 ± 5
Ni	none	39.5 ± 2.3	43.8 ± 2.9	36.6 ± 1.7	40.5 ± 2.5	39.2 ± 2.3	40.3 ± 0.5	37.5 ± 0.1
Pb	none	183 ± 8	203 ± 22	147 ± 6	208 ± 15	172 ± 15	193 ± 1	188 ± 9
V	none	133 ± 5	155 ± 9	129 ± 1	147 ± 8	141 ± 2	143 ± 2	140 ± 1
Al[a]	20 times	6.62 ± 0.32	5.07 ± 0.5	4.55 ± 1.0	4.12± 0.81	5.61 ± 0.3	3.41± 0.20	3.78 ± 0.2
Fe[a]	20 times	4.09 ± 0.06	3.56 ± 0.2	3.56 ± 0.2	4.03 ± 0.1	4.0 ±. 0.1	3.99± 0.10	3.95 ± 0.1
Cd	none	2.11 ± 0.15	1.98± 0.21	2.27± 0.12	2.71± 0.31	2.11±0.13	2.17± 0.10	2.35±0.13
Zn	none[b]	374 ± 23	332 ± 2	328 ± 17	362 ± 28	361 ± 31	353 ± 6	347 ± 16
Mn	20 times	440 ± 19	351 ± 35	354 ± 31	372 ± 16	412 ± 2	421 ± 3	429 ± 4
Ba	20 times	–	324 ± 10	412 ± 107	792 ± 166	893 ± 153	186 ± 13	219 ± 17

[a] Results are in % (w/w); the uncertainties are the standard deviations of 3 replicate measurements.

[b] 20 times diluted when alkaline fusion was used.

TABLE V
Analysis of Certified Marine Sediments Using Alkaline Fusion
Results in μg g^{-1} and the spectral lines listed in Table II were used.

Analyte	View	Sample Dilution	Certified	Found
Al[a]	Radial	20 times	6.62 ± 0.32	6.25 ± 0.15
Fe[a]	Radial	20 times	4.09 ± 0.06	4.01 ± 0.09
Zn	Radial	20 times	374 ± 23	413 ± 26
Mn	Radial	20 times	440 ± 19	428 ± 5
Ba	Radial	20 times	–	937 ± 4

[a] Results are in % (w/w); the uncertainties are the standard deviations
of 3 replicate measurements.

good results were only found for Al, Ba, Mn, Fe, and Zn using radial view. In this case, the use of axial view was not investigated in order to improve sensitivity due to the fact that Al, Ba, Mn, Fe, and Zn concentrations are relatively high in marine sediments. As expected, the alkaline fusion method, using open flasks, is not feasible for trace element determination mainly due to the high blank signal observed and analyte losses. Therefore, the analytes can be put into two groups for determination: As, Co, Cd, Cr, Ni, Pb, Cu, and V in the solution of the sample solubilized using method digestion 2 (Table III) and Al, Fe, Zn, Mn, and Ba in the solution of the alkaline sample fusion. The observation view as listed in Table II should be selected. Since only radial view was investigated for Al, Fe, Zn, Mn, and Ba determinations in the solution of the fused sample, this observation mode is recommended. However, if one decides to determine Zn, Mn, and Fe in the solution of the acid-digested sample by using method 2 (Table III), then both the radial and axial view can be used.

The limits of detection (LOD, 3 σ of 10 consecutive sample blank runs) and the relative standard deviations (% RSD) of 10 consecutive sample runs using the optimized method are described in Table VI. All analytes were measured in the solution of the solubilized sample using method digestion 2 (Table III). Al, Fe, Zn, Mn, and Ba were also measured in the solution of the fused sample. The results in Table

TABLE VI
Figures of Merit of the Proposed Method
Results in μg g^{-1}.

	As 188.979	Co 231.161	Cr 267.716	Cu 324.752	Ni 231.604	Pb 220.604	V 292.464	Al 396.153	Cd 228.802	Ba 455.403	Fe 239.562	Mn 257.610	Zn 213.857
LOD	1.68	2.76	0.62	2.06	0.84	2.21	0.78	0.86 *0.18	0.057	0.01 *0.01	0.03 *0.82	0.002 *0.005	0.004 0.035
%RSD	4.62	6.12	2.79	2.56	4.34	3.21	2.29	2.01 *2.08	5.80	1.93 *2.04	1.04 *1.10	1.18 *0.098	2.12 *2.15

View of observation: axial for As and radial for all other analytes.
*For the fused sample.
LOD= limit of detection (for all procedures).
%RSD= relative standard deviation.

TABLE VII
Real Marine Sediment Sample Analysis
Results in μg g^{-1} and spectral lines according to Table II were used.

Analyte	Sample 1	Sample 2	Sample 3	Sample 4	Sample 5	Sample 6	Sample 7	Sample 8
As	26.1± 0.14	30.4 ± 1,6	24.3 ± 1.8	50.2 ± 2,2	42.5 ± 3.7	36.2± 1.6	33.7 ± 1.2	34.4 ± 1.3
Co	9.80 ± 0.4	11.2± 0.08	9.72± 0.05	11.7± 0.30	10.8± 0.5	11.1±0.37	11.1±0.18	11.4± 0.40
Cr	75.9 ± 2.7	78.7 ± 1.6	68.6 ± 1.2	78.2 ± 3.0	81.0 ± 12	69.8 ± 5.4	69.6 ± 0.9	68.7 ± 1.7
Cu	16.9 ± 1.0	21.1 ±0.20	17.3 ±0.73	21.9 ± 1.5	20.6±0.30	22.2±0.85	22.8 ±0.55	21.7±0.27
Ni	33.7 ± 1.5	34.6 ±0.80	28.0 ± 1.8	36.8 ±0.87	36.1 ± 3.8	38.5 ± 1.4	38.9 ±0.73	37.2±0.86
Pb	28.6 ± 1.2	28.7 ±0.05	28.0 ±1.8	32.0 ± 1.0	28.4 ±1.3	27.1 ±1.3	30.7 ±0.83	28.1 ±1.6
V	98.4 ± 2.3	109 ± 1	96.2 ± 2.0	113 ± 4	105 ± 1	109 ± 4	116 ± 25	111 ± 2
Al[a]	4.86±0.32	2.25±0.09	1.74±0.01	2.46±0.01	2.31±0.07	4.85±1.36	4.05±0.14	3.36±0.26
Fe[a]	3.04± 0.05	3.27± 0.03	2.61± 0.04	3.57±0.19	3.43±0.01	4.25±0.30	3.66±0.13	3.92±0.14
Cd	0.29±0.05	0.37± 0.01	0.25± 0.02	0.42± 0.08	0.34±0.06	0.34±0.02	0.33±0.01	0.34±0.05
Zn	66.0 ± 2.9	71.0 ±0.60	59.7 ±0.30	70.5 ± 1.5	66.7±0.61	71.8 ± 3.0	70.1 ±0.25	69.6 ± 4.4
Mn	614±19	620±11	478±3.0	1386±58	1172±16	396±27	1258±7.0	862±21
Ba	410± 17	206± 6	206± 23	239± 15	221± 12	219± 18	368± 20	241± 28

[a] Results are in % (w/w); the uncertainties are the standard deviations of 3 replicate measurements.

VI show that precision is good since the RSD is lower than 5% for all analytes. Detection limits are also good, demonstrating the method's applicability for trace element determination in marine sediments.

The proposed method was also applied to the analysis of real samples and the results are listed in Table VII. It can be seen that the method is feasible for the determination of all analytes in real marine sediment samples.

CONCLUSION

The results obtained demonstrate that using axial and radial view provides good analytical results in the ICP-OES determination of trace and major elements in marine sediment samples. External calibration can be used to determine all investigated analytes. With the GemCone™ nebulizer (PerkinElmer), alumina injector, and Ryton® Scott spray chamber introducion of concentrated solutions into the plasma is possible, even when high amounts of the corrosive HF are present. The best sample decomposition method for Al and Ba determination is alkaline fusion, whereas acid digestion using a mixture of HF, HCl, and HNO_3 under pressure provides best results in the determination of As, Co, Cr, Cu, Ni, Pb, V, Fe, Cd, and Zn. Iron, Zn, and Mn can also be determined using alkaline fusion.

REFERENCES

1. Yun-chang Sun, Po-hsiang Chi, and Mei-yun Shiue, Anal. Sciences 17, 1395 (2001).

2. M. Bettinelli, G.M. Beone, S. Spezia, and C. Baffi, Anal. Chim. Acta 424, 289 (2000).

3. W. Diegor, H. Longerich, T. Abrajano, and I. Horn, Anal. Chim. Acta 431, 195 (2001).

4. C.R. Khorge, P. Chakrabarty, and R. Saran, At. Spectrosc. 21(6), 220 (2000).

5. R. Lara, R.A. Olsina, E. Marchevsky, J.A. Gásquez and L.D. Martinez, At. Spectrosc. 21(5), 172 (2000).

6. V.L. Dressler, D. Pozebon, and A.J. Curtius, Spectrochim. Acta B, 1527 (1998).

7. Khakhathi L. Mandiwana, J. Anal. At. Spectrom. 15, 1405 (2000).

8. D. Pozebon, V.L. Dressler, and A.J. Curtius, Talanta 51, 903 (2000).

9. Rong Wei and Hiroki Haraguchi, Anal. Sciences 15, 729 (1999).

10. K. Mitko and M. Bebek, At. Spectrosc. 21(3), 77 (2000).

11. R. Klockenkamper, F. Alt, and R. Brantd, J. Anal. At. Spectrom 16 (6), 658 (2001)

12. G.A. Zachariads, A.N. Anthemedis, I. Caniou, and J.A. Strates, International Journal of Environmental Analytical Chemistry 80 (3), 153 (2001).

13. P. Bermejo Barrera, M.C. Barciela Alonso, J.M. Moreda Pineiro, C. Gonzalez Sixto, and A. Bermejo Barrera, Spectrochim. Acta B, 51 (9-10), 1235 (1996).

14. R.S. Atgin, O. El-Algha, A. Zararsiz, A. Kocatas, H. Parlak, and G. Tuncel, Spectrochim. Acta B 55, 1151 (2000).

15. J.C. Ivaldi and J. F. Tyson, Spectrochim. Acta B 50, 1207 (1995).

16. M. Stepan, P. Musil, E. Poussel, and J.M. Mermet, Spectrochim. Acta B 56, 443 (2001).

17. M. Chausseau, E. Poussel, and J.M. Mermet, Fresenius' J. Anal Chem. 370, 341 (2001).

18. X. Romero, E. Poussel, and J. M. Mermet, Spectrochim. Acta B 52, 495 (1997).

Matrix Effects of Tantalum in the Determination of Cr, Fe, Nb, Ni, and Ti in Tantalum Powder Using ICP-OES

G. Anil, *M.R.P. Reddy, Arbind Kumar, and T.L. Prakash
Centre for Materials for Electronics Technology (C-MET)
IDA, Phase-II, HCL Post, Cherlapalli
Hyderabad - 500 051, India

INTRODUCTION

Inductively coupled plasma optical emission spectrometry (ICP-OES) is a widely used instrumental technique for the determination of a large number of analytes at different concentration levels. ICP-OES offers high sample throughput with a wide dynamic range and is relatively free from matrix interferences. A limiting factor of the technique which affects trace elemental analysis in the presence of complex matrices is due to the transfer of main matrix elements to the plasma at the same rate as that of the trace. This can result in changes in the plasma; thus adversely influencing the analysis.

Several research groups have conducted studies on the matrix interference effect, but the matrix elements studied have been restricted to alkali metals (1–9). In terms of mechanisms, matrix effects are due to ionization suppression by an excess of electrons from the easily ionizable elements (alkali metals) by increasing collision excitation as a result of the increased number of high-energy electrons. In the case of transitional elements (10,11), both atomic and ionic lines are suppressed in intensity in the presence of the interferent. This is due to ambipolar diffusion, a mechanism brought about by electrons diffusing radially out of the central channel. This would tend to drag positive ions away from the center to cause a reduction in the number of analyte

_____
*Corresponding author.
e-mail: mrpreddy@yahoo.com

ABSTRACT

Inductively coupled plasma optical emission spectrometry was applied to the determination of trace impurities in tantalum powder. The matrix effects of tantalum in the determination of trace level impurities such as Cr, Fe, Nb, Ni, and Ti were studied by measuring the intensities of each trace element in solution at various concentrations of tantalum. As the concentration of the interfering element increased, the trace sensitivity decreased similar to a linear decay, except for iron which showed a slight enhancement. The relative standard intensities of analytes in the tantalum matrix were calculated from 1000 to 20,000 mg/L tantalum solutions. The spectral line profile of the trace elements and the interference effects of tantalum at different concentrations are presented and discussed.

ions and, therefore, decrease analyte emission intensity in this region.

C-MET, Hyderabad, is actively involved in the preparation of low and high voltage capacitor-grade tantalum powder through solvent extraction and sodium reduction routes. Analysis of tantalum powder is routinely carried out using ICP-OES and many interferences are seen during the determination of Cr, Fe, Nb, Ni, and Ti. The present analytical work will be vital in regard to tantalum capacitor performance and applications.

EXPERIMENTAL

Instrumentation

The instrument used for the determination of trace elements in tantalum powder was a

Model JY-24R inductively coupled plasma optical emission spectrometer (ICP-OES) (Jobin Yvon, France). A cross-flow type nebulizer was used for pneumatic nebulization. The instrumental parameters are given in Table I.

Reagents and Standard Solutions

All chemicals used were of Suprapur® grade (Merck). The single elemental standard solutions were of Merck grade. The distilled deionized water used was prepared using the Nanopure system (Barnstead, USA).

Experimental Procedure

Tantalum powder was dissolved in a mixture of $HF + HNO_3$ and appropriate concentrations (ranging from 1000 to 20,000 mg/L) were prepared. Trace element standard solutions were mixed into the tantalum solution. To overcome analytical bias due to possible contamination of traces in the matrices, the matrix solution was analyzed as a blank for all trace element studies.

RESULTS AND DISCUSSION

Matrix-free Line Selection

The spectral interferences that commonly accompany the selection of analyte peaks are coincident line overlap, wing overlap from a much more intense line nearby, and broad-band background enhancement or background shift. These types of interferences can cause an added interference effect on the calibration function. In absolute terms, the bias caused by the tantalum concentration is independent of the analyte concentration.

TABLE I
ICP-OES Instrumental Operating Conditions

Sequential Spectrometer	Jobin Yvon JY-24R
	0.64-m Czerny-Turner
Grating	Holographic, 3600 grooves mm^{-1}
Spectral range	160-500 nm
Slit width	20 nm for entrance and exits, adjustable
HDD Detector	Dynamic range 2.5 x 10^{10}
Image	Measures complete emission spectrum in 2 min (230,000 points)
Plasma torch assembly	Fused quartz with capillary injection
Nebulizer and spray chamber	Cross-flow type nebulizer and Teflon® dual-tube spray chamber
Argon coolant gas flow rate	1.5 L min^{-1}
Argon plasma gas flow rate	12 L min^{-1}

TABLE II
Spectral Interference of Tantalum on Cr, Fe, Nb, Ni, and Ti Wavelengths
(1 mg/L of Cr, Fe, Nb, Ni, and Ti lines overlapped with 1000 mg/L of tantalum)

Wavelengths Cr	Wavelengths Fe	Wavelengths Nb	Wavelengths Ni	Wavelengths Ti
205.552 nm*	233.280 nm>	210.942 nm<	216.556 nm^	308.802 nm^
206.149 nm*	234.349 nm^	269.706 nm<	217.467 nm^	323.452 nm^
206.542 nm*	234.810 nm^	271.662 nm^	221.647 nm^	323.657 nm*
266.602 nm^	238.204 nm^	272.198 nm<	225.386 nm^	323.904 nm^
267.716 nm*	238.863 nm<	287.539 nm^	227.021 nm *	334.904 nm^
276.654 nm^	239.562 nm<>	288.318 nm*	230.300 nm^	334.941 nm^
283.563 nm*	240.488 nm^	292.781 nm^	231.604 nm^	336.121 nm*
284.325 nm<>	258.588 nm*	295.088 nm*	232.003 nm<>	337.280 nm*
284.984 nm^	259.940 nm^	309.418 nm^	234.554 nm^	338.376 nm^
286.257 nm*	261.187 nm^	313.079 nm^	341.476 nm*	368.520 nm*
286.511 nm>	263.105 nm<>	319.498 nm^	352.454 nm^	----
286.674 nm*	273.955 nm<	322.548 nm^	---	----
----	274.932 nm*	----	----	----
----	275.574 nm^	-----	-----	----

* : No tantalum line overlap present in the vicinity of ±0.05 nm.
^ : Direct tantalum line overlap.
<> : Right- and left-wing overlap of tantalum line.
> : Right-wing overlap of tantalum line.
< : Left-wing overlap of tantalum line.

Complex spectra are most troublesome during analysis when produced by the major constituent (i.e., tantalum) because spectral lines from tantalum tend to overlap lines of the analytes or traces. Line profiling was performed for each element and profiles of 1 mg/L Cr, Fe, Nb, Ni, and Ti standards were plotted and overlapped with 1000 mg/L tantalum individually. The spectral interference of tantalum on Cr, Fe, Nb, Ni, and Ti is given in Table II.

Chromium Lines

For selecting a chromium line free of tantalum interference, 12 high sensitivity lines were selected (12,13). Of the 12 lines, three lines (266.602 nm, 276.654 nm, and 284.984 nm) had a direct tantalum overlap, and two lines (284.352 nm and 286.511 nm) had a wing overlap of tantalum.

The spectral interference-free lines were 205.552 nm, 206.149 nm, 206.542 nm, 267.716 nm, 283.563 nm, 286.257 nm, and 286.674 nm.

Iron Lines

Fourteen high sensitivity lines were selected (12,13). Of 14 lines selected, seven lines (234.349 nm, 234.810 nm, 238.204 nm, 240.488 nm, 259.940 nm, 261.187 nm, and 275.574 nm) had a direct tantalum overlap and five lines (233.280 nm, 238.863 nm, 239.562 nm, 263.105 nm, and 273.955 nm) had a wing overlap of tantalum. The spectral interference-free lines were 258.588 nm and 274.932 nm.

Niobium Lines

Twelve high sensitivity lines were selected (12,13). Of 12 lines selected, seven lines (271.622 nm, 287.539 nm, 292.781 nm, 309.418 nm, 313.079 nm, 319.498 nm, and 322.548 nm) had a direct tantalum overlap and three lines (210.942 nm, 269.706 nm, and 272.198 nm) had a wing overlap of tantalum.

The spectral interference-free lines were 288.318 nm and 295.088 nm.

Nickel Lines

Eleven high sensitivity lines were selected (12,13). Of 11 lines selected, eight lines (216.556 nm, 217.467 nm, 221.647 nm, 225.386 nm, 230.300 nm, 231.604 nm, 234.554 nm, and 352.484 nm) had a direct tantalum overlap and 232.003 nm had a wing overlap. The spectral interference-free lines were 227.021 nm and 341.476 nm.

Titanium Lines

Ten high sensitivity lines were selected (12,13). Of 10 lines selected, six lines (308.802 nm, 323.452 nm, 323.904 nm, 334.904 nm, 334.941 nm, and 338.376 nm) had a direct tantalum overlap. The spectral interference-free lines were 323.657 nm, 336.121 nm, 337.280 nm, and 368.520 nm.

Tantalum-related Effects

Almost any matrix element can cause a change in the sensitivity of a susceptible spectral line. This effect is related to the ionization buffering of easily ionizing elements, such as sodium and potassium, which cause smaller effects than some elements with higher ionization potentials like tantalum. The effects are rather complicated and far from fully characterized. For any trace element line, the matrix effect is strongly related to the line excitation potential and the energy required to excite the trace element from its ground state, or a low-lying energy level, to the excited state. The analyte lines of Cr, Fe, Nb, Ni, and Ti have a high line excitation potential (i.e., the energy required to raise the analyte atom from its ground state, or low-lying energy level, to the excited state) and in the presence of tantalum are much more susceptible to matrix effects in comparison to elements such as calcium or potassium which have a low excitation potential.

Nevertheless, a grasp of the broad aspects is meaningful because it bears on the conduct of practical analysis. The influence of 1000 to 20,000 mg/L of tantalum on 1 mg/L of Cr, Fe, Nb, Ni, and Ti standards was studied.

In the case of chromium, except for 205.552 nm and 267.716 nm, other lines had spectral interferences from a tantalum line of tantalum concentrations greater than 2000 mg/L. The 205.552-nm line showed a decrease in intensity in the 5–25% range and the 267.716-nm line showed no change in intensity. Details of these results are given in Table III.

In the case of iron, the 258.588-nm line had a spectral interference from a tantalum line of tantalum concentrations greater than 5000 mg/L. The 274.932-nm line showed an increase in intensity in the 3–14% range. Details of these results are given in Table IV.

In the case of niobium, the 288.021-nm line had a spectral interference from a tantalum line at tantalum concentrations greater than 10,000 mg/L. The 295.088-nm line showed no decrease in intensity. Details of these results are given in Table V.

In the case of nickel, the 341.476-nm line had a spectral interference from a tantalum line at tantalum concentrations greater than 5000 mg/L. The 227.021-nm line showed a decrease in intensity in the 3–10% range. Details of these results are given in Table VI.

In the case of titanium, except for 336.121 nm and 337.280 nm, other lines had spectral interference from a tantalum line at tantalum concentrations greater than 5000 mg/L. The 336.121-nm line showed a decrease in intensity in the 2–4% range and the 337.280-nm line showed a decrease in intensity in the 2–9% range. Details of these results are given in Table VII.

Matrix Factor

A general matrix factor was calculated with the help of the analysis above. With a matrix factor, the trace element analysis in tantalum powder can be carried out with a pure standard rather than with a standard reference material (SRM); thus matrix-matching is not required.

Actual result = Experimental value x Matrix factor (for 1000–20,000 mg/L tantalum solutions)

Experimental value is the results obtained by analyzing the tantalum solution by ICP-OES.

Matrix factor (M) =100 / 100 ± increase/decrease in percentage at different concentrations

Standards in the range of 1 mg/L (Cr, Fe, Nb, Ni, and Ti) of the analyte were doped into standard solutions of tantalum in the range of 1000, 2000, 5000, 10,000, and 20,000 mg/L, respectively, and the increase or decrease in percentage of the analytes was calculated with respect to a pure standard.

Comparison of Results With a Certified Powder

The method developed was verified by analyzing 2 g each of certified tantalum powders STA-18KT (H.C. Starck GmbH & Co., K.G., Germany) and FTW-100 (Capacitor-grade powder, China) dissolved in 100 mL (i.e., 20,000 mg/L of tantalum). The results are presented in the Table VIII. In addition, a 2-g/100 mL of tantalum powder, spiked with pure standard solution of 0.25 mg/L and 0.5 mg/L Cr, Fe, Nb, Ni, and Ti, and the recovery percentage was calculated with and without a matrix factor.

TABLE III
Chromium (1 mg/L) Added to Different Ta Concentrations

Sample No.	Wavelength	1000 mg/L (S.D) Ta	2000 mg/L (S.D) Ta	5000 mg/L (S.D) Ta	10,000 mg/L (S.D) Ta	20,000 mg/L (S.D) Ta
1.	205.552 nm	0.95±0.010	0.92±0.015	0.88±0.020	0.81±0.020	0.75±0.018
2.	206.149 nm	0.92±0.010	0.82±0.035	0.73±0.021	CR	CR
3.	206.542 nm	0.98±0.008	0.83±0.033	CR	CR	CR
4.	267.716 nm	1.02±0.030	1.01±0.026	0.99±0.025	1.02±0.021	0.99±0.025
5.	283.563 nm	0.98±0.020	0.95±0.022	CR	CR	CR
6.	286.257 nm	0.93±0.020	CR	CR	CR	CR
7.	286.674 nm	0.91±0.030	0.99±0.031	CR	CR	CR

(S.D) : Standard Deviation of five readings.
C.R : Cannot be resolved at this concentration of tantalum.

TABLE IV
Iron (1 mg/L) Added to Different Ta Concentrations

Sample No.	Wavelength	1000 mg/L (S.D) Ta	2000 mg/L (S.D) Ta	5000 mg/L (S.D) Ta	10,000 mg/L (S.D) Ta	20,000 mg/L (S.D) Ta
1.	258.588 nm	0.84±0.010	0.79±0.02	CR	CR	CR
2.	274.932 nm	1.01±0.02	0.99±0.02	1.03±0.01	1.07±0.009	1.14±0.009

(S.D) : Standard Deviation of five readings.
C.R : Cannot be resolved at this concentration of tantalum.

TABLE V
Niobium (1 mg/L) Added to Different Ta Concentrations

Sample No.	Wavelength	1000 mg/L (S.D) Ta	2000 mg/L (S.D) Ta	5000 mg/L (S.D) Ta	10,000 mg/L (S.D) Ta	20,000 mg/L (S.D) Ta
1.	288.021 nm	1.01±0.002	1.02±0.010	0.99±0.012	0.99±0.010	CR
2.	295.088nm	0.98±0.002	0.99±0.005	0.99±0.003	1.01±0.004	1.00±0.004

(S.D) : Standard Deviation of five readings.
C.R : Cannot be resolved at this concentration of tantalum.

TABLE VI
Nickel (1 mg/L) Added to Different Ta Concentrations

Sample No.	Wavelength	1000 mg/L (S.D) Ta	2000 mg/L (S.D) Ta	5000 mg/L (S.D) Ta	10,000 mg/L (S.D) Ta	20,000 mg/L (S.D) Ta
1.	227.021 nm	0.97±0.010	0.97±0.010	0.95±0.020	0.92±0.025	0.90±0.025
2.	341.476 nm	1.04±0.010	1.08±0.010	CR	CR	CR

(S.D) : Standard Deviation of five readings.
C.R : Cannot be resolved at this concentration of tantalum.

TABLE VII
Titanium (1 mg/L) Added to Different Ta Concentrations

Sample No.	Wavelength	1000 mg/L (S.D) Ta	2000 mg/L (S.D) Ta	5000 mg/L (S.D) Ta	10,000 mg/L (S.D) Ta	20,000 mg/L (S.D) Ta
1.	323.657 nm	0.98±0.010	0.99±0.012	0.98±0.011	CR	CR
2.	336.121 nm	1.01±0.008	1.01±0.003	0.98±0.007	0.98±0.02	0.96 ±0.005
3.	337.280 nm	0.98±0.010	0.98±0.005	0.95±0.002	0.92±0.008	0.91±0.005
4.	368.520 nm	0.99±0.010	0.90±0.006	CR	CR	CR

(S.D) : Standard Deviation of five readings.

C.R : Cannot be resolved at this concentration of tantalum.

TABLE VIII
Analysis of Certified Powders
(Results in mg/L)

Sample No.	Elements	Wavelength	Certified Values (STA-18KT)	Experimental Results X Matrix Factor (STA-18KT)	Certified Values (FTW-100)	Experimental Results Matrix Factor (FTW-100)
1.	Chromium	267.716 nm	<2.0	1.62 X 1 =1.62	9	8.67 X 1 = 8.67
2.	Iron	274.932 nm	7.0	8.05 X 0.925 = 7.43	24	26.5 X 0.925 = 24.51
3.	Niobium	295.088 nm	<1.0	0.66 X 1 = 0.66	N.R	0.88 X 1 = 0.88
4.	Nickel	227.021 nm	6.0	5.50 X 1.11 = 6.10	10	9.41 X 1.11 = 10.44

N.R: Values not reported.

TABLE IX
Recovery of 0.25 mg/L and 0.50 mg/L Cr, Fe, Nb, Ni & Ti
Spiked in 2 g/100 mL Tantalum Powder

Sample No.	Elements	Wavelength	0.25 mg/L spiked Cr, Fe, Nb, Ni & Ti		0.5 mg/L spiked Cr, Fe, Nb, Ni & Ti	
			Recovery % without matrix factor calculation (SD)	Recovery % with matrix factor calculation (SD)	Recovery % without matrix factor calculation (SD)	Recovery % with matrix factor calculation (SD)
1.	Chromium	267.716 nm	99.28± 0.10	100.06±0.05	99.12±0.07	100.05±0.03
2.	Iron	274.932 nm	114.32±0.09	100.18±0.08	114.18±0.06	100.10±0.06
3.	Niobium	295.088 nm	100.21±0.11	100.09±0.06	100.09±0.05	100.12±0.04
4.	Nickel	227.021 nm	90.38±0.08	100.05±0.04	90.23±0.06	100.09±0.07
5.	Titanium	336.121 nm	96.18±0.05	100.12±0.06	96.11±0.09	100.10±0.06

(S.D) : Standard Deviation of five readings.

The results are presented in Table IX. From these experiments it can be inferred that the experimental values, when multiplied using the matrix factor, showed very close proximity to the certified values as well as with the recovery results of spiked analytes.

CONCLUSION

The ICP-OES, having a 0.64 m monochromator, was successfully applied to the determination of trace elements Cr, Fe, Nb, Ni, and Ti in tantalum powder by selecting lines for each element that are free from tantalum interferences and calculating the matrix effects factor of tantalum ranging from 1000 mg/L to 20,000 mg/L tantalum. This factor was applied to the analysis of certified material and found to be very suitable. The method described can be applied universally for the determination of trace elements in tantalum powder.

REFERENCES

1. M.F. Zaranyika and A.T. Chirenje, Fresenius' J. Anal. Chem. 368, 45 (2000).

2. M.F. Zaranyika and A.T. Chirenje, Fresenius' J. Anal. Chem. 364, 208 (1999).

3. Jan LM de Boer, Walter van Leeuwen, Ute Kohlmeyer, and M. Peter Breugem, Freseniusí J. Anal. Chem. 360, 213 (1998).

4. I.B. Brenner, A. Zander, M. Cole, and A. Wiseman, J. Anal. At. Spectrom. 12, 897 (1997).

5. L. Paama and P. Peramaki, At. Spectrosc. 18, 119 (1997).

6. A.D. Klerk and C. Rademeyer, J. Anal. At. Spectrom. 12, 1221 (1997).

7. Wing-Tat Chan, George CY Chan, Zhenbin Gong, and Nick MN Fan, Analytical Sciences 12, 235 (2000).

8. M. Villaneuva, M. Catasus, E.E. Salin, and M. Pomares, J. Anal. At. Spectrom. 15, 877 (2000).

9. A. Krejcova, T. Cernohorsky, and E. Curdova, J. Anal. At. Spectrom. 16, 1002 (2001).

10. R.M. Tripkovic, D. Ivanka, and Holclajtner-Antunovic, J. Anal. At. Spectrom. 8, 349 (1993).

11. D. Ivanka, Holclajtner-Antunovic, and R.M. Tripkovic, J. Anal. At. Spectrom. 8, 359 (1993).

12. A. Montaser and D.W. Golightly, Inductively Coupled Plasmas in Analytical Spectrometry, Second Edition, VCH Publishers, Inc. (1992).

13. R. Payling and P. Larkins, Optical Emission Lines of the Elements, John Wiley and Sons Ltd., New York (2000).